Proceedings of the 6th IEEE International
Conference on Nano/Molecular Medicine and Engineering
November 4-7, 2012, Bangkok, Thailand

# A Microfluidic Biosensor for Multiplexed Detection of Bacterial Pathogens

Peter B. Lillehoj
Department of Mechanical Engineering
Michigan State University
East Lansing, MI U.S.A.
E-mail: lillehoj@egr.msu.edu

Chih-Ming Ho[1] and Wenyuan Shi[2]
[1]UCLA, Mechanical & Aerospace Engineering Department
[2]UCLA School of Dentistry
Los Angeles, CA U.S.A.

Chis Kaplan and Jian He
C3 Jian, Inc.
Inglewood, CA U.S.A.

***Abstract*—The detection of bacterial pathogens has far-reaching impacts in various applications including food safety, water quality monitoring and clinical diagnosis. Owing to this, ongoing efforts have focused on developing biodetectors that are portable, offer rapid measurements and high specificity. Here, we present a microfluidic biosensor capable of fast, multiplexed detection of bacterial pathogens. This device utilizes a microsensor array patterned with synthetic, antimicrobial peptides that have species-specific targeting and binding capabilities. The peptides utilized in this work target for two species of bacterium; *Streptococcus mutans* and *Pseudomonas aeruginosa*, which are major sources of disease and infection in humans. Samples are autonomously driven within the device via a hydrophilic poly(dimethylsiloxane) PDMS surface coating. An electrical impedance sensing scheme is utilized for cell detection where cell binding results in changes of the sensor's impedance. Using this device, *S. mutans* and *P. aeruginosa* cells could be simultaneously detected in a polymicrobial sample within 20 min, demonstrating its potential as a rapid, point-of-care diagnostic technology.**

***Index Terms*—Microfluidic biosensor, impedance detection, antimicrobial peptides (AMPs), bacterial pathogens**

## I. Introduction

Bacterial pathogens residing within human mucosal surfaces, such as the mouth, stomach and gut, play a crucial role in maintaining healthy immune functionality [1-3]. Recent studies have shown a strong correlation between the presence of specific oral pathogens in the body to the development of various systemic illnesses including diabetes, cardiovascular disease, kidney disease and respiratory disease [4, 5]. Therefore, the detection of relevant bacteria in salvia can provide a novel, non-invasive means for disease diagnosis and health monitoring. Conventional approaches for detecting pathogenic bacteria include enzyme-linked immunosorbent assay (ELISA) and polymerase chain reaction (PCR) [6, 7]. Microsensor-based devices have also been developed [8-10] for bacteria detection. However, most of these technologies rely on antibodies for biorecognition, which have limited stability and shelf life. Additionally, antibodies lack the ability to specifically target individual species within diverse cell populations, limiting its effectiveness for detection in complex clinical samples (roughly 500-1000 species of bacteria reside in the human body) [11]. In contrast, antimicrobial peptides (AMPs) demonstrate high stability [12, 13] and selectivity, making them suitable as biorecognition elements for sensing. Recent works have utilized AMPs for fluorescent- [14] and electrical-based [15] detection of bacteria. However, a rapid, portable biodetector that is capable of highly-selective, multiplexed pathogen detection in clinical samples has yet to be developed. We present a microfluidic biosensing platform that can simultaneously target and rapidly detect multiple disease-causing pathogens utilizing selectively-targeted AMPs [16-18] in a mixed cell solution.

Briefly, our device consists of a microsensor array coupled with a poly(dimethylsiloxane) (PDMS) fluidic network (Fig 1). The microsensors are patterned with synthetic AMPs that contain a C-terminus cysteine residue, enabling for thiol-gold binding. An electrical impedance sensing scheme is utilized which allows for rapid, label-free cell detection, circumventing the need for bulky optical equipment and complicated processing steps (e.g. cell lysis, amplification, fluorescent tagging) required for other detection methods [19]. A hydrophilic surface treatment is applied to the PDMS chip [20] enabling for fluids to be autonomously driven via capillary pumping, thereby eliminating the need for external pumps and minimizing the overall size of the system. Using this device, *P. aeruginosa* and *S. mutans* cells could be simultaneous detected within a polymicrobial sample. Impedance measurements are completed within 5 sec and the entire detection process, including sample loading, incubation and sensing, can be completed within 20 min. Ultimately, this device presents an enabling technology for advancing microsensor-based diagnostics by providing a portable, highly-specific, in situ test for quickly detecting disease-causing pathogens in clinical samples.

## II. Materials & Methods

### *A. Device Fabrication & Assembly*

PDMS molds were fabricated on Si wafers via photolithography (Karl Suss) and DRIE (Unaxis). A PDMS mixture (Sylgard 184) was poured onto the mold, cured for 2 hr at 80°C, cut into individual chips, and inlet and outlet holes were punched. A hydrophilic surface coating was applied to the PDMS chips as previously reported [20]. The fabrication of the microsensor array consisted of photolithography to

978-1-4673-5103-4/12/$31.00 © 2012 IEEE

pattern AZ4620 photoresist as a shadow mask for metal evaporation. Cr and Au were evaporated (CHA Mark 40) onto glass slides (Fisher Scientific) and then lift-off was performed via sonication in acetone. Devices were assembled by bonding together the PDMS and glass chips, which were rinsed in isopropanol and DI water and dried in compressed $N_2$. Device assembly was performed under a microscope to ensure that the channels were properly aligned with the microsensor array.

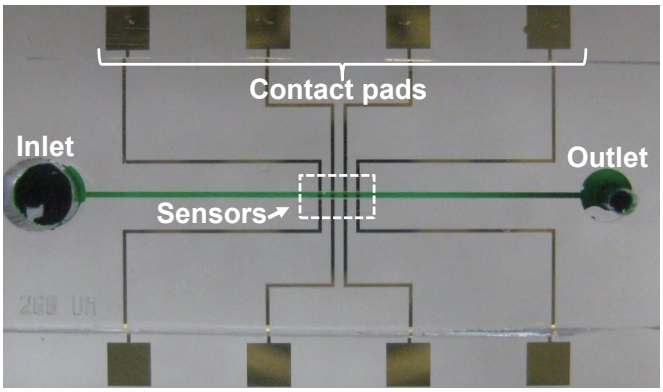


Fig. 1. Photograph of the device. The microchannel is filled with dye for enhanced visualization. The microsensor array is outlined in white.

*B. Peptide Immobilization*

A second PDMS chips was utilized for peptide immobilization. This chip incorporates 4 individual microchannels which are designed to flow over the center electrodes of the sensors without crossing over the contact leads (Fig. 2). Peptide solutions were manually dispensed into the inlets of the device using a pipette and pumped through the channel using a syringe. After 15 min incubation, the peptide solutions were flushed out of the channels, followed by subsequent rinsing in DI water. The PDMS chip was detached from the microsensor array, which was rinsed in DI water and dried using compressed $N_2$.

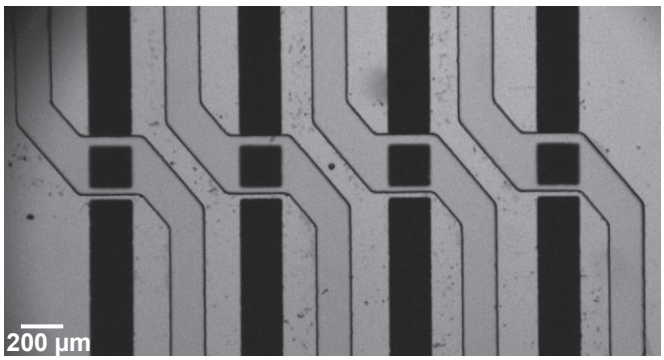


Fig. 2. Image of the microfluidic network for peptide immobilization. Microchannels, 200 µm in width, expand to 300 µm when passing over the middle electrodes of the sensors. Sensors are shown in black.

*C. Cell Culture & Peptide Preparation*

*S. mutans* were grown in brain heart infusion (BHI) or Todd-Hewitt (TH) medium (Difco) at 37°C under anaerobic conditions (80% N2, 10% CO2, and 10% H2) [18]. *P. aeruginosa* were grown in Luria-Bertani (LB) broth medium (Fisher Scientific) at 37°C under aerobic conditions. The AMPs used in this work are named C16G2cys and G10KHc, which were synthesized and purified using previously established techniques [16, 17]. The amino acid sequences of these peptides are:

C16G2cys (targets *S. mutans*):
TFFRLFNRSFTQALGKGGGKNLRIIRKGIHIIKKYGGGC

G10KHc (targets *P. aeruginosa*):
KKHRKHRKHRKHGGSGGSKNLRRIIRKGIHIIKKYGC

Peptide solutions were generated by dissolving peptide resins in 50% DI water and 50% methanol to a concentration of 5 µM. Peptide solutions were stored at -17°C and thawed to room temperature prior to experiments.

*D. Microscopic Imaging*

Device assembly was performed under a Leica microscope (DM4000M) equipped with a CoolSNAPHQ Monochrome CCD camera (Photometrics, Tucson, AZ). Peptide immobilization and cell binding was visualized using fluorescence microscopy. Images were captured using RS Image software. Fluorescent images were processed (imaging stacking, contrast enhancement) using ImageJ software (open source, NIH).

*E. AFM Imaging*

Surface topologies were captured in air using a Digital Instruments MultiMode Scanning Probe Microscope (SPM) with a Nanoscope 3A controller (Santa Barbara, CA) operating in tapping mode. Specimens were mounted to steel discs, which were magnetically attached to the stage. Silicon probes (Veeco Probes, Camarillo, CA) were used with a typical tapping frequency of 240–280 kHz and a nominal scanning rate of 0.8–1.0 Hz. Images were analyzed and processed using Digital Instruments Nanoscope R IIIa software.

*F. Impedance Measurements*

An electrical impedance sensing scheme is utilized for cell detection. Electrical impedance measurements were carried out using a 4294A precision impedance analyzer (Agilent, Palo Alto, CA), which can perform measurements in a broad-frequency range from 40 Hz to 110 MHz with an impedance accuracy of ± 0.08%. Kynar wiring (30 AWG) was used to connect the impedance analyzer to the devices. Spring-loaded connector pins (Digi-Key, Thief River Falls, MN) were soldered at one end of the wires, facilitating contact to the electrodes. A custom polycarbonate chip holder was fabricated using a MAXNC 15 computer numerical controlled (CNC) mill. After securing the device in the holder, a solution of mixed cells was pumped into the microchannel. Prior to measurements, the samples were incubated in the channel for 15 min to allow for cell binding. Next, phosphate buffered saline (PBS, Fisher Scientific) was pumped inside the microchannel to flush out unbound cells. After 3 rinsing cycles, fresh PBS was pumped into the device for impedance

measurements. A 100 mV excitation voltage was applied for all measurements and the impedance was scanned from 100 Hz to 100 MHz in a logarithmic scale with 200 data points for each scan. Impedance measurements were taken in PBS (pH 7.2, EC 38 mS/cm). Each measurement lasted 5 sec.

## III. Results & Discussion

### *A. Characterization of Peptide Immobilization*

AFM scans were performed to characterize the binding of the peptides to the sensor. Peptide solutions, at a concentration of 1 µM, were incubated on Au surfaces for 15 min, rinsed with a DI/methanol solution and dried using compressed $N_2$. As shown in Figure 3, peptides can be clearly observed on the Au surface. Specifically, the 3D scan reveals that the peptides are vertically aligned, validating that binding occurs at the C-terminus (at the cysteine residue). Since the sequences of both peptides do not contain additional cysteine molecules, the probability for misalignment is minimized. The vertical arrangement of the peptides is crucial for effective cell recognition and binding. Topographic data also suggests that the peptides are arranged vertically; peptides aggregates measure ~16 nm in height, matching closely with measurements of similar-sized peptides [21]. The peptides also demonstrate strong surface binding, being able to withstand repeated rinsing in DI/methanol solution. From these results, it can be determined that the unique design of these peptides enables for optimal surface alignment, surface uniformity and binding strength.

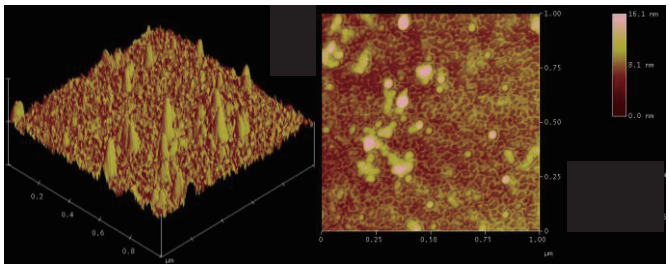

Fig. 3. AFM scans of peptides immobilized on Au. The scan size and z-scale are 1 µm x 1 µm and 16 nm respectively.

### *B. Characterization the Impedance Sensor*

Impedance measurements of NaCl solutions having various molar concentrations were performed to characterize the response of the system. As shown in Figure 4, different concentration solutions generated distinctive impedance spectra. Based on this plot, we observe that the largest shift in the impedance occurs at the middle frequency range ($f_{middle}$), between 10 kHz and 1 MHz. Specifically, the lowest concentration solution (0.001 M) exhibits the largest impedance (~200 kΩ at $f_{middle}$) due to it having the lowest electrical conductivity. Solutions with higher NaCl concentrations exhibit lower impedances owing to their higher conductivities, which facilitates the flow of current within the solution. Interestingly, the data shows a strong correlation between the magnitudes of the impedance (at $f_{middle}$) and the solution concentration (i.e., the change in impedance occurs at a similar order of magnitude with the corresponding solution concentration).

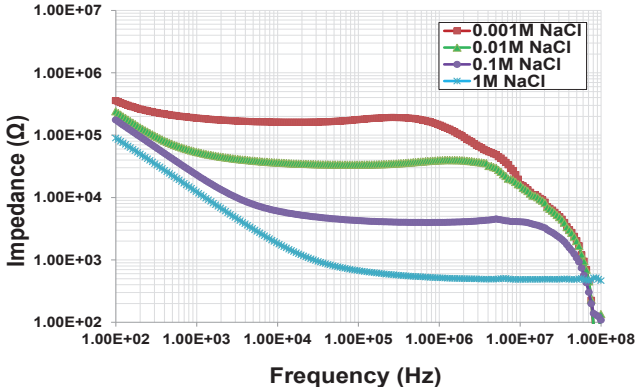


Fig. 4. Impedance spectra of NaCl solutions at various concentrations. Higher concentration solutions exhibit decreasing impedance with spectra profiles shifted toward the upper frequency regime.

### *C. Cell Targeting and Binding*

Binding assays against G10KHc- and C16G2cys-coated sensors were performed using fluorescently labeled *S. mutans* and *P. aeruginosa* cells. Sensors were coated with 2 different peptides: sensors S1 and S2 were coated with G10KHc and sensors S3 and S4 were coated with C16G2cys. A solution containing a mixture of *S. mutans* and *P. aeruginosa* was pumped inside the microchannel and incubated for 15 min (Fig. 5A). The solution was flushed out and rinsed with PBS 3 times to remove unbound cells. As shown in Fig. 5B, the remaining florescent signals indicate cells bound to the sensors. Sensors S1 and S2 exhibit strong preferential binding to *P. aeruginosa* (stained red) with negligible binding to *S. mutans* (stained green). Similarly, sensors S3 and S4 exhibit preferential binding to *S. mutans* with negligible binding to *P. aeruginosa*. Additionally, it can be observed that bound cells are localized within the sensor regions (outlined in white) signifying that there is minimal cross- and non-specific binding. These results demonstrate the high specificity and strong binding properties of these peptides, making them well-suited as biorecognition elements.

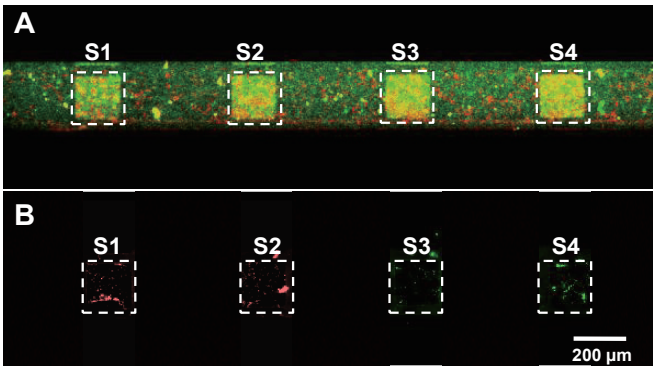


Fig. 5. Fluorescence images of (A) the cell solution flowing inside the microchannel and (B) captured cells on the sensors. Sensors S1 and S2 are coated with G10KHc and sensors S3 and S4 are coated with C16G2cys. The solution contains a mixture of *S. mutans* (labeled green) and *P. aeruginosa* (labeled red) suspended in PBS. The electrodes are outlined in white.

### D. Cell Detection

As shown in Fig. 6, sensors containing *S. mutans* and *P. aeruginosa* cells generated clearly distinguishable impedance spectra compared with control measurements (uncoated sensors containing no cells). Two sensors were coated with the same peptide and two separate measurements were taken at each sensor to obtain replicate data. Based on these plots, we can see that each pair of sensors generated nearly identical impedance spectra along the entire frequency sweep. For both cell types, the change in impedance from the control measurements was the greatest at the lower frequency range ($f_{lower}$, $10^2$ – $10^4$ Hz). Specifically, sensors containing bound cells exhibited impedances 4x larger (~90 kΩ at $10^2$ Hz) compared with the control measurements. At higher frequencies, the change in the impedance became negligible until ~$10^4$ Hz, where the signals are indistinguishable from the control.

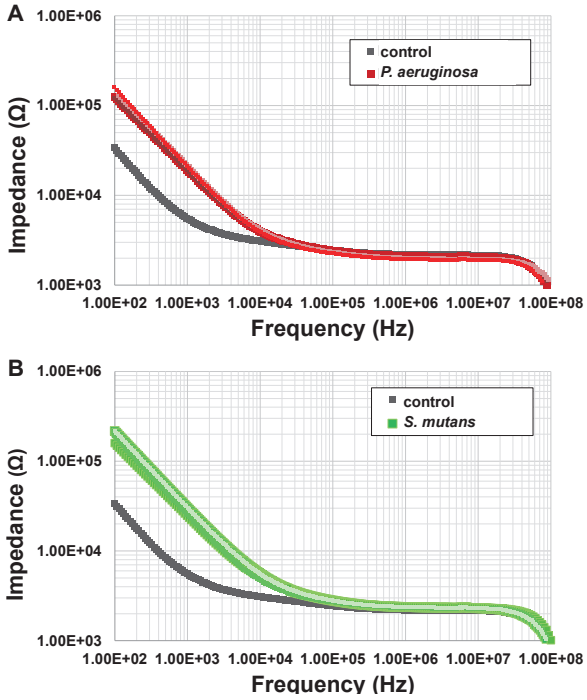


Fig. 6. Impedance spectra of sensors with bound cells; (A) *P. aeruginosa* and (B) *S. mutans*. Control measurements were performed on uncoated sensors containing no cells. Each plot is comprised four individual cell measurements.

## IV. Conclusions

We have presented a microfluidic biosensor for rapid and multiplexed detection of bacterial pathogens. This platform utilizes robust AMPs, which are designed with highly-specific targeting and binding capabilities. Peptides were patterned onto Au microsensors via thiol-gold binding, which resulted in a vertical orientation and strong surface binding. Binding assays were performed on peptide-coated sensors with a mixture of fluorescently labeled *S. mutans* and *P. aeruginosa* cells. Based on these experiments, peptide-coated sensors demonstrated strong preferential binding to their corresponding targeted cells with negligible cross-binding. An electrical impedance sensing scheme was utilized to detect cells; sensors with bound cells exhibited impedances 4x larger compared with the control measurements. Additionally, each measurement requires only 5 sec and the entire detection process could be completed within 20 min. Further development of this device would entail implementing additional sensors to detect for other pathogenic bacteria (e.g. *Campylobacter*, *Salmonella*), enhancing its versatility and diagnostic capabilities. Ultimately, this platform demonstrates the immense potential of AMP-based electric biosensors, which can provide rapid, highly-specific, multiplexed detection for point-of-care diagnosis and health monitoring.

## Acknowledgments

This work was generously funded by the following agencies: NASA National Space Biomedical Research Institute (NCC 9-58-317), UCLA T32 Dentist-Scientist & Oral Health Scientist Training Program (DE 007296) and the Bill and Melinda Gates Foundation (442561-HC-80086).

## References

[1] H. G. Boman, "Innate immunity and the normal microflora," Immuno. Rev., vol. 173, pp. 5 – 16, 2000.

[2] K. M. Pickard, A. R. Bremmer, J. N. Gordon and T. T. MacDonald, "Microbial-gut interactions in health and disease. Immune responses." Best Prac. Res. Cl. Ga., vol. 18, pp. 271 – 285, 2004.

[3] I. Sekirov, S. L. Russell, L. C. M. Antunes and B. B. Finlay, "Gut microbiota in health and disease," Phys. Rev., vol. 90, pp. 859 – 904, 2010.

[4] X. Li, K. M. Kolltveit, L. Tronstad and I. Olsen, "Systemic diseases caused by oral infection," Clin. Microbio. Rev., vol. 13, pp. 547 – 558, 2000.

[5] R. I. Garcia, M. M. Henshaw and E. A. Krall, "Relationship between periodontal disease and systemic health," Peridontol., vol. 25, pp. 21 – 36, 2001.

[6] P. Daly, T. Collier and S. Doyle, "PCR-ELISA detection of *Escherichia coli* in milk," Lett. Appl. Microbiol., vol. 34, pp. 222 – 226, 2002.

[7] P. R. Johnson et al., "Detection of *Escherichia coli* O157:H7 in meat by an enzyme-linked immunosorbent assay EHEC-tek," Appl. Environ. Microbiol., vol. 61, pp. 386 – 388, 1995.

[8] S. M. Radke and E. C. Alocilja, "A high density microelectrode array biosensor for detection of *E. coli* O157:H7," Biosen. Bioelectron., vol. 20, pp. 1662 – 1667, 2005.

[9] S. T. Pathirana et al., "Rapid and sensitive biosensor for *Salmonella*" Biosen. Bioelectron., vol. 15, pp. 135 – 141, 2000.

[10] D. A. Boehm et al., "On-chip microfluidic biosensor for bacterial detection and identification," Sensor Actuat. B-Chem., vol. 126, pp. 508 – 514, 2007.

[11] C. L. Sears, "A dynamic partnership: celebrating our gut flora," Anaerobe, vol. 11, pp. 247 – 251, 2005.

[12] C. Friedrich, M. G. Scott, N. Karunaratne, H. Yan and R. E. W. Hancock, "Salt-resistant alphahelical cationic antimicrobial

peptides," Antimicrob. Agents Chemother., vol. 43, pp. 1542 – 1548, 1999.

[13] T. Rydlo, S. Rotem and A. Mor, "Antibacterial properties of dermaseptin S4 derivatives under extreme incubation conditions," Antimicrob. Agents Chemother., vol. 50, pp. 490 – 497, 2006.

[14] N. V. Kulagina, K. M. Shaffer, G. P. Anderson, F. S. Ligler and C. R. Taitt, "Antimicrobial peptide-based array for *Escherichia coli* and *Salmonella* screening," Anal. Chim. Acta, vol. 575 pp. 9 – 15, 2006.

[15] M. S. Manoor, S. Zhang, A. J. Link and M. C. McAlpine, "Electrical detection of pathogenic bacteria via immobilized antimicrobial peptides," Proc. Natl. Acad. Sci. USA, vol. 107, pp. 19207 – 19212, 2010.

[16] J. He, et al., "Novel synthetic antimicrobial peptides against *Streptococcus mutans*," Antimicrob. Agents Chemother., vol. 51, pp. 1351 – 1358, 2007.

[17] R. Eckert, et al., "Adding selectivity to antimicrobial peptides: Rational design of a multidomain peptide against *Pseudomonas spp*.," Antimicrob. Agents Chemother., vol. 50, pp. 1480 – 1488, 2006.

[18] R. Eckert, et al., "Targeted killing of *Streptococcus mutans* by a pheromone-guided "smart" antimicrobial peptide," Antimicrob. Agents Chemther., vol. 50, pp. 3651 – 3657, 2006.

[19] D. Ivnitski et al., "Biosensors for detection of pathogenic bacteria," Biosen. Bioelectron., vol. 14, pp. 599 – 624, 1999.

[20] P. B. Lillehoj and C.-M. Ho, "A long-term, stable hydrophilic poly(dimethylsiloxane) coating for capillary-based pumping," in Proc. of 23rd IEEE MEMS 2010, pp. 1063 – 1066, 2010.

[21] T. Kowalewski and D. M. Holtzman, "In situ atomic force microscopy study of Alzheimer's beta-amyloid peptide on different substrates: New insights into mechanism of beta-sheet formation," Proc. Natl. Acad. Sci. USA, vol. 96, pp. 3688 – 3693, 1999.